Chemical Physics 524 (2019) 101–105

Contents lists available at ScienceDirect

Chemical Physics

journal homepage: www.elsevier.com/locate/chemphys

Tuning the electronic properties of GaS monolayer by strain engineering and electric field

Khang D. Pham[a,b], Vo T.T. Vi[c], Doan V. Thuan[d,*], Nguyen V. Hieu[e], Chuong V. Nguyen[f], Huynh V. Phuc[g], Bui D. Hoi[c], Le T.T. Phuong[c], Nguyen Q. Cuong[c], Dung V. Lu[e], Nguyen N. Hieu[h,*]

[a] Laboratory of Applied Physics, Advanced Institute of Materials Science, Ton Duc Thang University, Ho Chi Minh City, Viet Nam
[b] Faculty of Applied Sciences, Ton Duc Thang University, Ho Chi Minh City, Viet Nam
[c] Department of Physics, University of Education, Hue University, Hue, Viet Nam
[d] NTT Hi-Tech Institute, Nguyen Tat Thanh University, Ho Chi Minh City, Viet Nam
[e] Department of Physics, University of Education, The University of Da Nang, Da Nang, Viet Nam
[f] Department of Materials Science and Engineering, Le Quy Don Technical University, Ha Noi, Viet Nam
[g] Division of Theoretical Physics, Dong Thap University, Cao Lanh, Viet Nam
[h] Institute of Research and Development, Duy Tan University, Da Nang, Viet Nam

ARTICLE INFO

Keywords:
GaS monolayer
Strain engineering
Electric field
Electronic properties
First-principles study

ABSTRACT

In the present study, the effects of the strain engineering and electric field on electronic properties of the GaS monolayer are investigated by *ab initio* investigations. Our calculated results demonstrate that the GaS monolayer is a semi-conductor with a large indirect bandgap of 2.568 eV at the equilibrium. In the presence of a biaxial strain, the band structure of the GaS monolayer, especially the conduction band, changes significantly. However, while the effect of compressive strain on the energy gap of the GaS monolayer is quite weak, its energy gap depends strongly on the tensile strain. On the other hand, external electric fields can cause the semiconductor–metal transition in the monolayer. Being able to control electronic properties, especially the occurrence of the semiconductor–metal phase transition, makes the GaS monolayer a prospective material for nanoelectromechanical and nanospintronic applications.

1. Introduction

Discovery of graphene [1] and its success in nandevices [2,3] has opened a deep revolution in the development of two-dimensional (2D) nanomaterials. With thousands of articles annually [4], graphene has become the hottest material of the material-related scientific community for nearly 15 years. However, in the form of semimetal with zero energy gap, one has seen that graphene has many incompatibilities with semiconductor technology as well as widely used silicon materials. In parallel with overcoming this disadvantage of graphene, scientists have begun a new journey to explore other 2D materials. From graphene-like materials, such as silicene [5,6], phosphorene [7,8] or transition metal dichalcogenides [9–11], to monochalcogenide materials [12], 2D layered materials have been particularly interested in over a decade due to their outstanding physical and chemical properties. Van der Waals heterostructures based on monochalcogenides or dichalcogenides have also been extensively studied [13–16]. Recently, monolayer monochalcogenides, especially the compounds with a wide bandgap, are particularly noticeable because they have many potential applications in opto-electronic devices [17,18].

Gallium sulfide (GaS) is one of the layered materials belonging to III–VI compounds. Atoms within the layers of the GaS are bonded by strong ionic-covalent bonds and GaS layers in bulk structure are held together by weak van der Waals (vdW) force. Since the interactions between layers are weak vdW forces, one believed that it is possible to separate monolayers from bulk materials by simple experimental methods. The GaS nanosheets have been successfully synthesized recently by several experimental methods [19–21]. In contrast to 2D single-layer graphene, a gapless semiconductor leading to many limitations in nanoelectronic applications [22], the previous study has shown that GaS monolayer is an excellent nanomaterial for field effect transistor applications [23]. Structural and electronic properties of the GaS monolayer have been considered by density functional theory (DFT) [24–26]. The GaS monolayer at equilibrium is a semiconductor with an energy gap of about 2.5 eV and one can control its bandgap easily by strain engineering [25,27]. Also, Yagmurcukardes and his

* Corresponding authors.
E-mail addresses: phamdinhkhang@tdtu.edu.vn (K.D. Pham), dvthuan@ntt.edu.vn (D.V. Thuan), hieunn@duytan.edu.vn (N.N. Hieu).

https://doi.org/10.1016/j.chemphys.2019.05.008
Received 3 April 2019; Received in revised form 9 May 2019; Accepted 10 May 2019
Available online 13 May 2019

group demonstrated that the GaS monolayer has an outstanding mechanical property that its structure can withstand strain up to 17% and semiconductor–metal phase transition can be found in the GaS monolayer at large biaxial strain [27].

In this work, we consider the electronic properties of the GaS monolayer under the electric field E and biaxial strain ε_b using first-principles calculations. Our calculations have been focused on the effect of the ε_b and E on the bandgap and band structures of the GaS monolayer. The role of strain ε_b and external field E in controlling the electronic properties of the GaS monolayer has also been investigated and discussed seriously.

2. Computational methods

All numerical calculations in this study were performed using the Quantum Espresso package [28] based on the accurate projector augmented-wave (PAW) method [29,30] with the generalized gradient approximation of the Perdew-Burke-Ernzerhof (PBE) exchange–correlation energy functional [31]. The Dispersion-corrected DFT with London dispersion corrections (PBE + D2) [32] has been used to consider the van der Waals (vdW) forces that may occur between Ga and S layers. The Brillouin zone in our calculations is represented by a $(15 \times 15 \times 1)k$-mesh Monkhorst-Pack grid. Energy of 500 eV was used as the kinetic energy cut-off for the plane-wave basis for all calculations. The structure of the GaS monolayer was fully relaxed with total energy and force convergence criteria being 10^{-6} eV and 0.01 eV/Å, respectively. To prevent interaction between neighboring monolayers, a large vacuum spacing of 20 Å was used.

When the biaxial strain is applied, we use the definition of the biaxial strain as $\varepsilon_b = (a - a_0)/a_0$, where a and a_0 are respectively the strained and unstrained lattice constants of the GaS monolayer. To estimate the influence of an external electric field $\vec{E}$ on the system, we applied the $\vec{E}$ perpendicular to the 2D surface of the GaS.

3. Results and discussion

GaS monolayer has a honeycomb structure formed from four sublayers of atoms stacked in order of S–Ga–Ga–S as illustrated in Fig. 1. Geometrically, the structure of the GaS monolayer belongs to the D_{3h} space group. Unit cell of the monolayer GaS contains four atoms, including two Ga atoms and two S atoms. At equilibrium, the lattice parameter of the GaS monolayer is 3.585 Å. Our calculated result is in good agreement with previous DFT studies [25,24]. We next examine the dynamical stability of the GaS monolayer structure by calculating its phonon dispersion curves. Our DFT calculations demonstrated that the phonon spectrum of the GaS monolayer has 12 branches, including nine optical branches and three acoustic branches as shown in Fig. 1(c). We clearly see that in the phonon dispersion of the GaS monolayer there are no imaginary frequencies (soft modes). It means that the structure

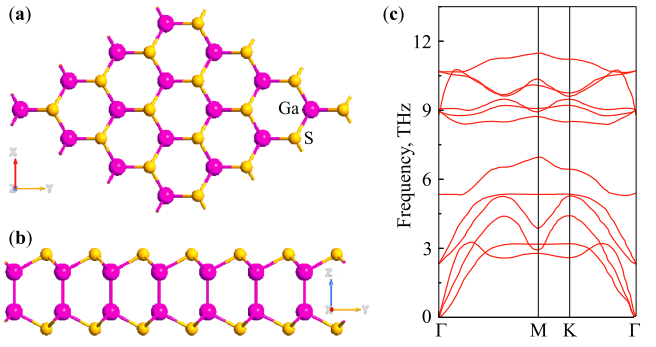

Fig. 1. Top (a) and side views (b) of GaS monolayer structure at equilibrium. (c) Phonon dispersion curves of the GaS monolayer.

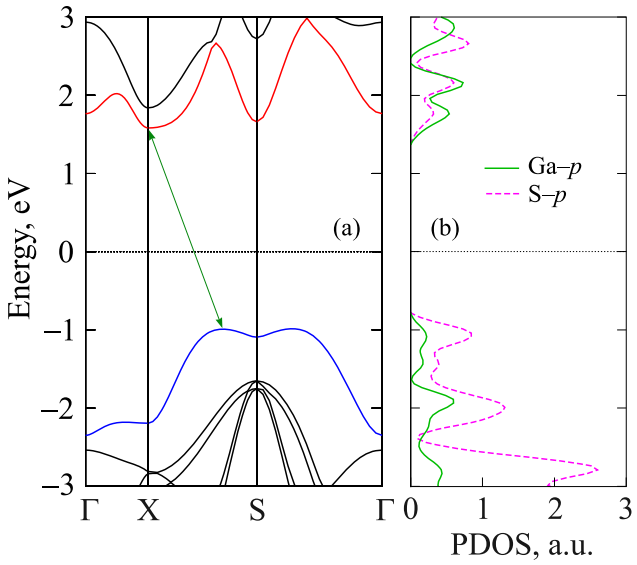

Fig. 2. Band structure (a) and PDOS (b) of GaS monolayer at equilibrium.

of the GaS monolayer is stable.

Our calculated results indicate that the total energy of the GaS monolayer at equilibrium is − 9370.19 eV. Focusing on the electronic properties of the monolayer of GaS, we first calculate the band structures and the partial density of states (PDOS) of the GaS monolayer at the equilibrium state as shown in Fig. 2. Clearly, we can see that, at equilibrium, the GaS monolayer is a semiconductor with a quite large indirect bandgap of 2.568 eV. This calculated result matches with the previous DFT simulations [27]. This bandgap value of GaS monolayer is greater than that of bulk material (1.59 eV) [33]. Also, Hu and his colleagues also demonstrated that the band gap and carrier mobility of gallium sulfide depends highly on the thickness of the material[33]. However, the bandgap problem of the nanomaterials depends largely on the approach in DFT calculations, i.e., energy functionals. For example, the energy gap of the GaS monolayer is up to 3.19 eV when it is estimated by using Hey–Scuseria–Ernzerhof fucntional (HSE06) [25]. However, physically, using different functionals in the DFT calculations only gives different bandgap values, not changing the basic physical properties of the material.

The indirect bandgap of the GaS monolayer at equilibrium formed by the conductor band minimum (CBM) located at X-point and the valence band maximum (VBM) lying on the XS-path (Fig. 2). Looking at the lowest energy subband in the conduction band (CB), we see that although the CBM is located at X-point, the difference in energy of the electronic states of the valence band (VB) at the X-, S-, and Γ-point is quite small. With such a small difference in energy of the electronic states of the VB, we believe that the band structures of the GaS monolayer can be greatly altered under the influence of strain ε_b or external field E. To clearly see the formation of energy bands of the GaS monolayer, we calculated the PDOS as shown in Fig. 2(b). The DFT calculations indicated that the s-orbitals to the electronic bands of the GaS monolayer is negligible. Both the CB and VB of the GaS monolayer are greatly donated by the Ga-p and S-p orbitals. While the contribution of the Ga-p and S-p orbitals to the CB is quite balanced, the VB is largely contributed by the S-p orbitals compared to Ga-p orbital's contribution.

For applications in the design technology of devices, such as in nanoelectromechanical devices or sensors, studying the change in electronic properties due to external impacts such as deformation or external fields is essential. Capturing the changing law of material properties due to these impacts allows us to have many options for applying it to specific devices. In order to study the influence of a strain engineering on electronic properties of the GaS monolayer, a biaxial strain ε_b varying from −10% to 10% is applied perpendicularly to the

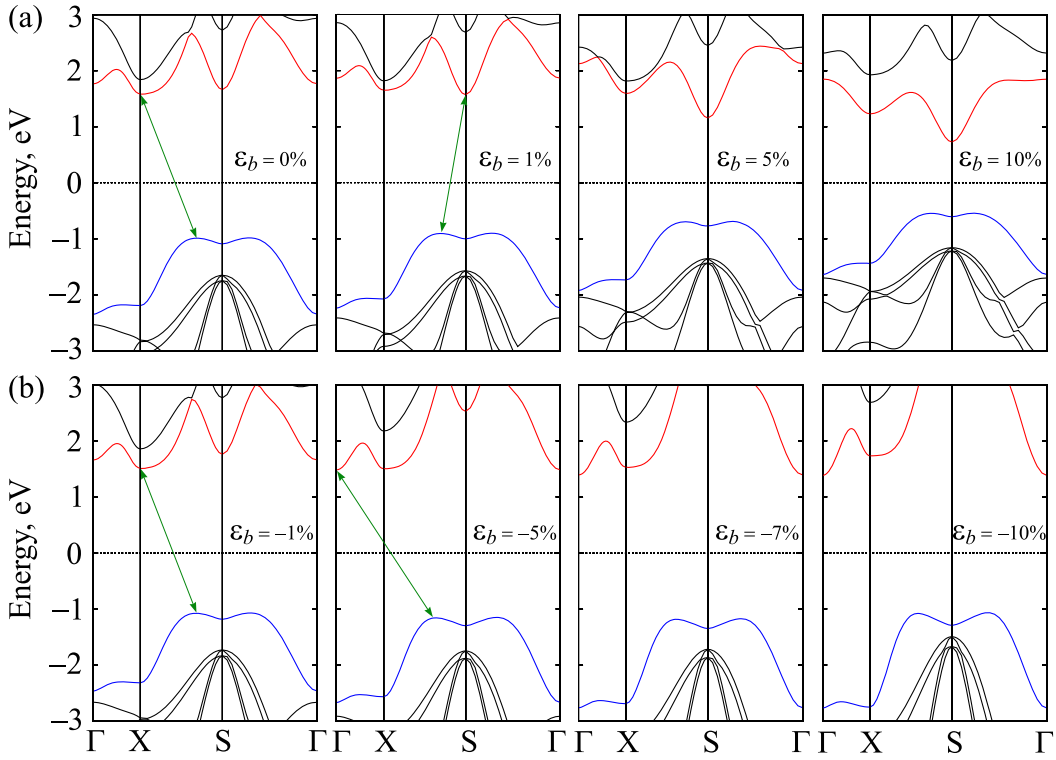

Fig. 3. Band structures of GaS monolayer under tensile (a) and compressive (b) biaxial strain ε_b.

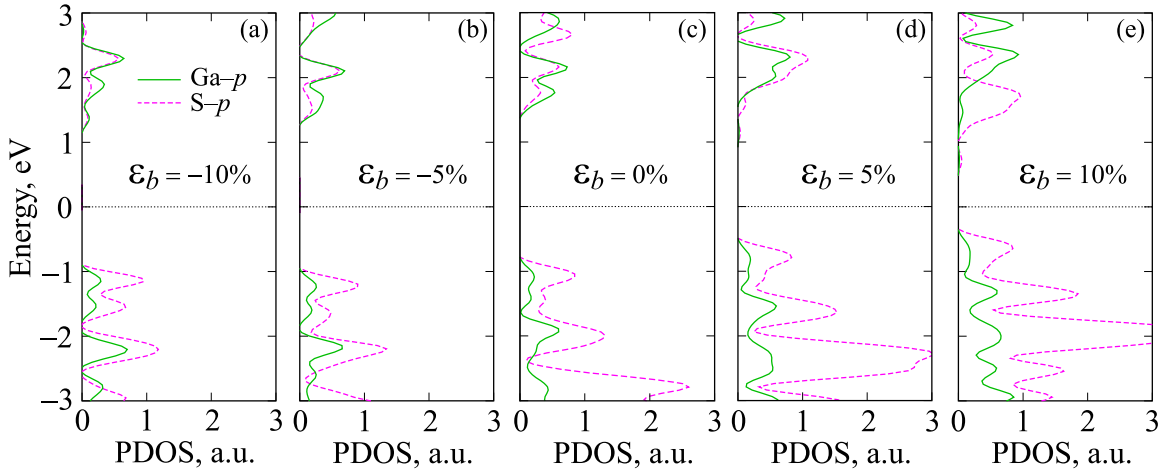

Fig. 4. PDOS of the monolayer GaS under different levels of biaxial strain ε_b: (a) $\varepsilon_b = -10\%$, (b) $\varepsilon_b = -5\%$, (c) $\varepsilon_b = 0\%$, (d) $\varepsilon_b = 5\%$, and (e) $\varepsilon_b = 10\%$.

two-dimensional surface of the GaS monolayer. The "+" and "−" signs refer respectively to the tensile and compressive cases of the biaxial strain. When a biaxial strain ε_b is applied, our calculated results indicated that the energy dispersion relations of the GaS monolayer have significant changes, especially the conduction band. In Fig. 3, we show the band structures of the strained GaS monolayer at different levels of ε_b. From Fig. 3, we see that, while the highest sub-band shape of the valence band is almost unchanged in the presence of the ε_b, the strain engineering causes great changes to the conduction band. Indeed, as shown in Fig. 3(a), we see that the position of the CBM has been changed from the X-point to S-point immediately when the tensile biaxial strain ($\varepsilon_b > 0$) is applied. In the case of compression biaxial strain, we see that the position change of CBM has also occurred. Our calculations show that the position of the CMB has shifted from the X-point to Γ-point at − 5% of the applied compressive biaxial strain as shown in Fig. 3(b). These changes of the CBM due to strain lead to a change in bandgap because the VBM is changed very little due to strain, particularly in the compressive biaxial strain case. To comprehensively see the contribution of orbitals to the electronic states of the GaS monolayer under strain engineering, we calculated the PDOS of the monolayer under several levels of biaxial strain as shown in Fig. 4. Our calculated results indicated that, compared to the contribution of the Ga-*p* orbitals, the contribution of the S-*p* orbitals to the valence band of monolayer GaS is outstanding, especially in the case of tensile biaxial strain. Meanwhile, the contribution of both the Ga-*p* and S-*p* orbitals to the conduction band is quite balanced in both cases of compressive and tensile strains. Fig. 5 shows the strain-dependence of the monolayer bandgap. Our calculated results indicated that while the effect of compressive biaxial strain on the bandgap E_g of the monolayer GaS is quite weak, the E_g of the monolayer depends greatly on the tensile biaxial strain. This downward trend of energy is in agreement with the previously calculated results, that the bandgap of the monolayer drops

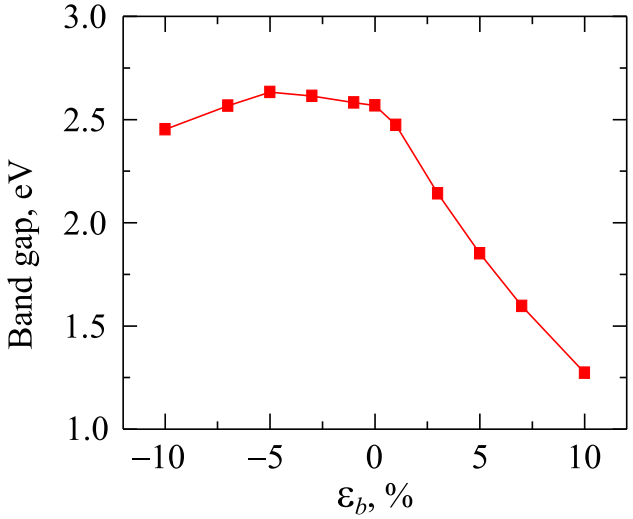

Fig. 5. Dependence of bandgap of GaS monolayer on biaxial strain ε_b.

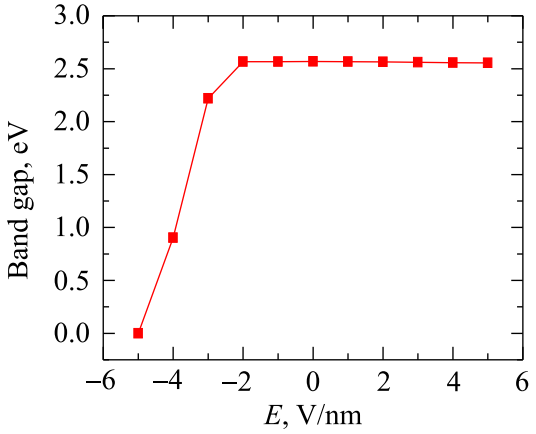

Fig. 7. Effect of electric field E on the bandgap of the GaS monolayer.

to zero at ε_b = 17%[27].

We next consider the influence of a perpendicular electric field E on the electronic properties of the GaS monolayer. To investigate the electronic properties of the GaS monolayer under the electric field, the electric field E is applied perpendicularly to the 2D plane of the monolayer. The investigated electric field varies from − 5 V/nm to 5 V/nm. The positive direction of the $\vec{E}$ is along with the positive direction of the z-axis. The negative electric field is implied that its direction is opposite to the positive direction of the z-axis. Band structures of the GaS monolayer under an external field is shown in Fig. 6. In Fig. 6(b), we showed that the position of CBM has moved from X-point to S-point at $E = -3$ V/nm. At the same time, when the negative electric field continues to increase, the bandgap of the GaS monolayer decreases rapidly and reaches zero at $E = -5$ V/nm. It means that the semiconductor–metal phase transition has occurred due to the presence of the external field. The modulation of the energy gap of the GaS monolayer via the external field E is shown in Fig. 7. It is clear that the band gap of the monolayer GaS depends weakly on the positive electric field. Our calculated results indicated that the band gap of the monolayer GaS is 2.568 eV and 2.555 eV at E = 0 V/nm and E = 5 V/nm, respectively. The band gap of the monolayer GaS tends to decrease when increasing the positive electric field, however, the difference in the energy gap of the monolayer GaS at different values of the positive electric fields is too small. This slight decrease in band gap by electric field has also been reported in previous studies for monolayer GaS [34] or similar materials such as InSe monolayer [35]. While the effect of the positive electric field on the band structures of the GaS monolayer is quite weak, the negative electric field is a key factor in tuning its electronic properties. It is clear that the bandgap decreases quite suddenly when we increase the intensity of the negative electric field. Clearly, the electronic properties of the GaS monolayer, especially bandgap, depend not only on the intensity of the external field E but also greatly on its direction. The total charge density of the monolayer GaS is also shown in Fig. 8. Being able to control the electronic properties of GaS monolayer with electric fields and especially the

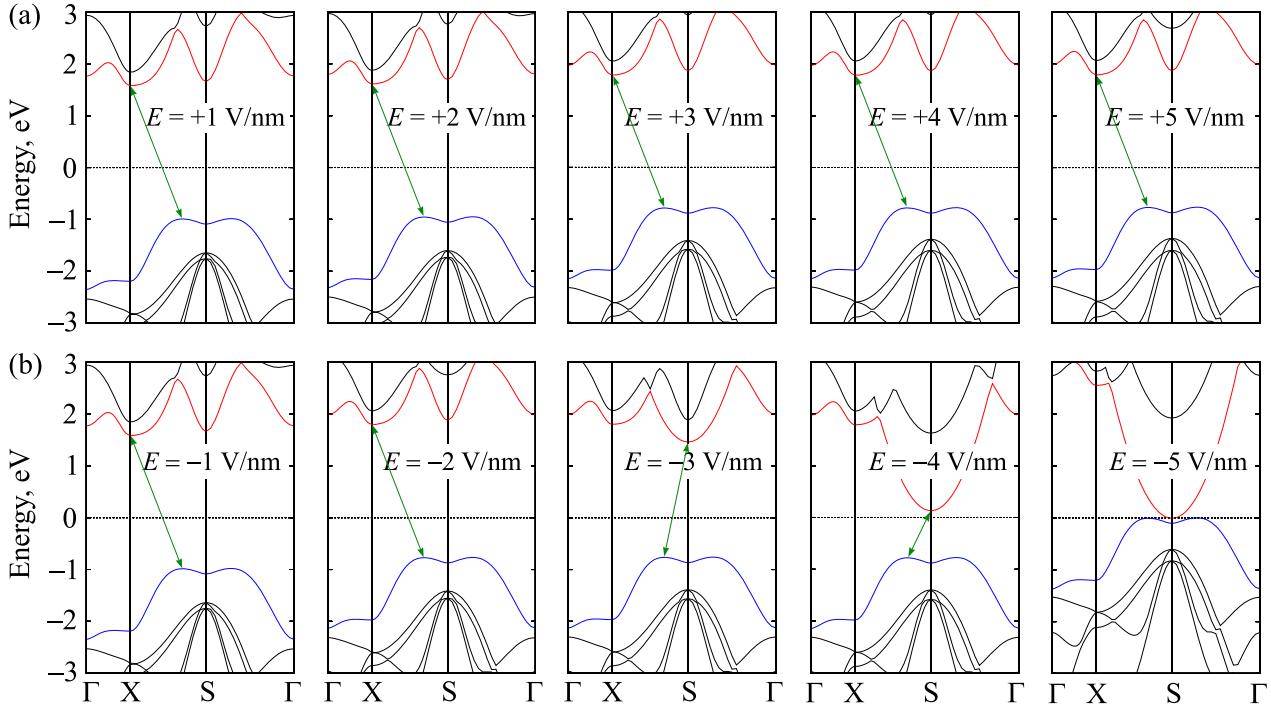

Fig. 6. Band structures of the GaS monolayer under the positive electric field $E > 0$ (a) and negative electric field $E < 0$ (b).

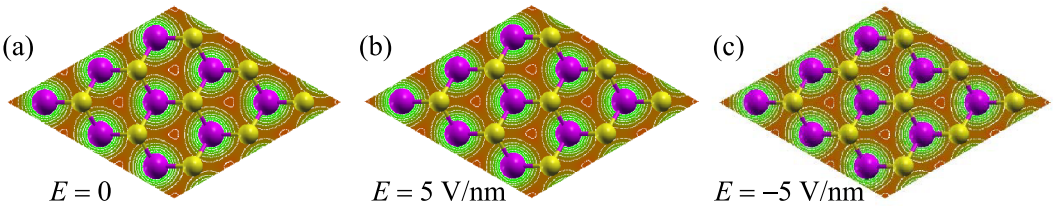

Fig. 8. Total charge density of the monolayer GaS under external electric field of (a) $E = 0$, (b) $E = 5$ V/nm, and (c) $E = -5$ V/nm.

appearance of the semiconductor–metal phase transition due to the external field can open up the possibility of applying it in nanoelectronic devices.

4. Conclusion

In conclusion, we have systematically considered the electronic properties of the GaS monolayer under the biaxial strain ε_b and electric field E using DFT calculations. Our calculated results indicated that the electronic properties of the GaS monolayer depend strongly on the biaxial strain and electric field, especially the tensile biaxial strain and negative external electric field. Also, the bandgap of the GaS monolayer can be easily modulated by applied strain or electric field making it a prospective material for applications in nanodevices. Our calculated results also contribute to an insightful view o the electronic properties of this two-dimensional material.

Declaration of Competing Interest

The authors declare that they have no conflict of interest.

Acknowledgment

This research is funded by the Vietnam National Foundation for Science and Technology Development (NAFOSTED) under Grant No. 103.01-2017.309.

References

[1] K.S. Novoselov, A.K. Geim, S.V. Morozov, D. Jiang, Y. Zhang, S.V. Dubonos, I.V. Grigorieva, A.A. Firsov, Science 306 (2004) 666.
[2] Y.-M. Lin, K.A. Jenkins, A. Valdes-Garcia, J.P. Small, D.B. Farmer, P. Avouris, Nano Lett. 9 (2009) 422.
[3] Y. Zheng, G.-X. Ni, C.-T. Toh, M.-G. Zeng, S.-T. Chen, K. Yao, B. Özyilmaz, Appl. Phys. Lett. 94 (2009) 163505.
[4] E.P. Randviir, D.A. Brownson, C.E. Banks, Mater. Today 17 (2014) 426.
[5] B. Lalmi, H. Oughaddou, H. Enriquez, A. Kara, S. Vizzini, B. Ealet, B. Aufray, Appl. Phys. Lett. 97 (2010) 223109.
[6] M. Yarmohammadi, Phys. Lett. A 381 (2017) 1261.
[7] P.T.T. Le, K. Mirabbaszadeh, M. Davoudiniya, M. Yarmohammadi, Phys. Chem. Chem. Phys. 20 (2018) 25044.
[8] H. Bui, M. Yarmohammadi, J. Magn. Magn. Mater. 465 (2018) 646.
[9] J.N. Coleman, M. Lotya, A. O'Neill, S.D. Bergin, P.J. King, U. Khan, K. Young, A. Gaucher, S. De, R.J. Smith, I.V. Shvets, S.K. Arora, G. Stanton, H.-Y. Kim, K. Lee, G.T. Kim, G.S. Duesberg, T. Hallam, J.J. Boland, J.J. Wang, J.F. Donegan, J.C. Grunlan, G. Moriarty, A. Shmeliov, R.J. Nicholls, J.M. Perkins, E.M. Grieveson, K. Theuwissen, D.W. McComb, P.D. Nellist, V. Nicolosi, Science 331 (2011) 568.
[10] M. Yarmohammadi, J. Magn. Magn. Mater. 426 (2017) 621.
[11] B.D. Hoi, M. Yarmohammadi, J. Magn. Magn. Mater. 451 (2018) 57.
[12] D.J. Late, B. Liu, H.S.S.R. Matte, C.N.R. Rao, V.P. Dravid, Adv. Funct. Mater. 22 (2012) 1894.
[13] P.T.T. Le, N.N. Hieu, L.M. Bui, H.V. Phuc, B.D. Hoi, B. Amin, C.V. Nguyen, Phys. Chem. Chem. Phys. 20 (2018) 27856.
[14] H.V. Phuc, N.N. Hieu, B.D. Hoi, C.V. Nguyen, Phys. Chem. Chem. Phys. 20 (2018) 17899.
[15] K.D. Pham, N.N. Hieu, H.V. Phuc, I.A. Fedorov, C.A. Duque, B. Amin, C.V. Nguyen, Appl. Phys. Lett. 113 (2018) 171605.
[16] K.D. Pham, C.V. Nguyen, H.T. Phung, H.V. Phuc, B. Amin, N.N. Hieu, Chem. Phys. 521 (2019) 92.
[17] Z. Wang, K. Xu, Y. Li, X. Zhan, M. Safdar, Q. Wang, F. Wang, J. He, ACS Nano 8 (2014) 4859.
[18] S. Zhou, C.-C. Liu, J. Zhao, Y. Yao, NPJ Quantum Mater. 3 (2018) 16.
[19] C.H. Ho, S.L. Lin, J. Appl. Phys. 100 (2006) 083508.
[20] A. Harvey, C. Backes, Z. Gholamvand, D. Hanlon, D. McAteer, H.C. Nerl, E. McGuire, A. Seral-Ascaso, Q.M. Ramasse, N. McEvoy, S. Winters, N.C. Berner, D. McCloskey, J.F. Donegan, G.S. Duesberg, V. Nicolosi, J.N. Coleman, Chem. Mater. 27 (2015) 3483.
[21] G. Shen, D. Chen, P.-C. Chen, C. Zhou, ACS Nano 3 (2009) 1115.
[22] F. Schwierz, Nat. Nanotechnol. 5 (2010) 487.
[23] D.J. Late, L. Bin, L. Jiajun, Y. Aiming, H.S.S. Ramakrishna Matte, G. Matthew, C.N.R. Rao, P. Dravid Vinayak, Adv. Mater. 24 (2012) 3549.
[24] Y. Ma, Y. Dai, M. Guo, L. Yu, B. Huang, Phys. Chem. Chem. Phys. 15 (2013) 7098.
[25] L. Huang, Z. Chen, J. Li, RSC Adv. 5 (2015) 5788.
[26] S. Demirci, N. Avazli, E. Durgun, S. Cahangirov, Phys. Rev. B 95 (2017) 115409.
[27] M. Yagmurcukardes, R.T. Senger, F.M. Peeters, H. Sahin, Phys. Rev. B 94 (2016) 245407.
[28] P. Giannozzi, S. Baroni, N. Bonini, M. Calandra, R. Car, C. Cavazzoni, D. Ceresoli, G.L. Chiarotti, M. Cococcioni, I. Dabo, A.D. Corso, S. de Gironcoli, S. Fabris, G. Fratesi, R. Gebauer, U. Gerstmann, C. Gougoussis, A. Kokalj, M. Lazzeri, L. Martin-Samos, N. Marzari, F. Mauri, R. Mazzarello, S. Paolini, A. Pasquarello, L. Paulatto, C. Sbraccia, S. Scandolo, G. Sclauzero, A.P. Seitsonen, A. Smogunov, P. Umari, R.M. Wentzcovitch, J. Phys.: Condens. Matter 21 (2009) 395502.
[29] P.E. Blöchl, Phys. Rev. B 50 (1994) 17953.
[30] G. Kresse, D. Joubert, Phys. Rev. B 59 (1999) 1758.
[31] J.P. Perdew, K. Burke, M. Ernzerhof, Phys. Rev. Lett. 77 (1996) 3865.
[32] S. Grimme, J. Comput. Chem. 27 (2006) 1787.
[33] P. Hu, L. Wang, M. Yoon, J. Zhang, W. Feng, X. Wang, Z. Wen, J.C. Idrobo, Y. Miyamoto, D.B. Geohegan, K. Xiao, Nano Lett. 13 (2013) 1649.
[34] F. Guo, Y. Wu, Z. Wu, C. Ke, C. Zhou, T. Chen, H. Li, C. Zhang, M. Fu, J. Kang, Nanoscale Res. Lett. 12 (2017) 409.
[35] X.-P. Wang, X.-B. Li, N.-K. Chen, J.-H. Zhao, Q.-D. Chen, H.-B. Sun, Phys. Chem. Chem. Phys. 20 (2018) 6945.